A truncated [MnIII 12] tetrahedron from oxime-based [MnIII 3O] building blocks

A Truncated $[Mn^{III}_{12}]$ Tetrahedron from Oxime-based $[Mn^{III}_{3}O]$ Building Blocks

J. M. Frost, S. Sanz, T. Rajeshkumar, M. B. Pitak, S. J. Coles, G. Rajaraman,* W. Wernsdorfer, J. Schnack,* P. J. Lusby and E. K. Brechin*

The use of the novel pro-ligand H_4L combining the complimentary phenolic oxime and diethanolamine moieties in one organic framework, results in the formation of the first example of a $[Mn^{III}_{12}]$ truncated tetrahedron and an extremely rare example of a Mn cage conforming to an Archimedean solid.

Synthetic coordination chemists have had enormous success in constructing large and aesthetically pleasing molecules containing paramagnetic metal ions, despite the many experimental difficulties in doing so.[1] In small nuclearity clusters the coordination sites of the metal ions can often be filled by design through the use of one polydentate ligand or through simple combinations of different ligand types, *e.g.* one bridging and one chelating ligand.[2-6] However, as the nuclearity of the cluster increases the structural complexity increases dramatically, the central cores often consist of numerous bridging oxide and/or hydroxide ions whose presence, number and coordination behaviour is difficult to predict, and the peripheral skin of the cage is adorned by numerous (often different) organic bridging ligands coordinating in a variety of ways, with solvent molecules filling what vacant metal sites remain.[7-14] As such almost all large cages of paramagnetic metal ions are heteroleptic in nature and require the use of complementary ligands in [serendipitous] self-assembly. One way of achieving future success in this regard is to mine structural databases to discover and then exploit the known coordination modes of certain ligand types. A particular ligand will often form the same metal–organic moiety under a variety of reaction conditions, and it is how these building blocks assemble that dictates the nature of the final product. Different ligands will of course form different building blocks and thus the combination of different ligands that produce complementary building blocks should produce beautiful new cages. Instead of employing these as two different reaction ingredients, we have been exploring a synthetic approach that combines these ligands into one structural framework, and two appealing candidates in this regard are the phenolic oximes[15] and the diethanolamines,[16] both of which have long and distinguished track records in cluster formation. Herein we report the synthesis, structure and magnetic behaviour of the truncated tetrahedron $[Mn^{III}_{12}O_4(H_3L)_8(H_2L)_4(TMA)_4]$ (**1**) constructed using the novel pro-ligand H_4L (Figure 1).

Reaction of $MnBr_2{\cdot}4H_2O$, H_4L and trimesic acid (H_3TMA) in a basic MeOH solution results in the formation of black rod-like crystals after slow evaporation of the filtered mother liquor, after 5 days (see the SI for full details). The crystals were in a tetragonal crystal system and structure solution was obtained in the $I4_1/a$ space group.

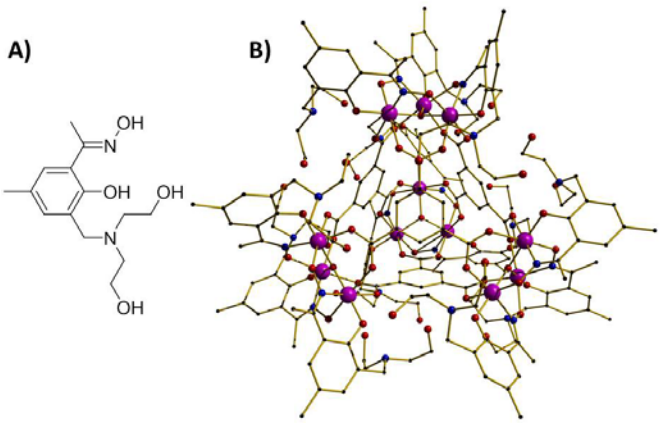

Figure 1. (A) The pro-ligand H_4L. (B) The molecular structure of **1**. Colour code: Mn = purple, O = red, N = blue, C = grey. H atoms have been omitted for clarity.

The metallic skeleton of **1** describes a truncated tetrahedron (or simply a tetrahedron if one considers the $[Mn_3]$ triangles as nodes) in which $[Mn^{III}_{3}O]^{7+}$ triangles occupy the vertices and the four μ_6-TMA^{3-} ligands panel the faces of the cage (Figures 1-2). The μ_3-O^{2-} ions lie at the centres of the $[Mn^{III}_{3}O]^{7+}$ triangles, slightly below the $[Mn_3]$ plane toward the centre of the cage (0.216 – 0.233 Å). The H_3L^- and H_2L^{2-} ligands employ their -N-O- oxime moieties to each bridge across one edge of a $[Mn_3]$ triangle, with each Mn-N-O-Mn moiety lying above the $[Mn_3]$ plane (Figure 2E) and pointing away from the centre of the cage. This in contrast to that observed in all phenolic-oxime based $[Mn_3]$ and $[Mn_6]$ molecules in which these moieties lie in the $[Mn_3]$ plane.[15] Interestingly, however, the same $[Mn^{III}_{3}O(NO)_3(O_2CR)_3]$ units have been observed in triangles stabilised with pyridyl oximes.[17] The phenolic O-atoms are terminally bonded. There are two sets of symmetry equivalent triangles in **1** (Mn1-Mn3, Mn4-Mn6; see the SI for crystallographic information) which, although appearing identical in nature are strictly scalene by definition. Although the Mn…Mn distances all fall within a very narrow range (3.214-3.247 Å for Mn1-3 and 3.223-3.233 Å for Mn4-6) there are three rather different and distinct Mn-N-O-Mn torsion angles (11.59, 18.91 and 23.90° for Mn1-3; 8.04, 16.57 and 23.43° for Mn4-6). The diethanolamine arms of the ligand remain non-bonded, and are involved in a myriad of H-bonding interactions O(diethanolamine)…O(diethanolamine), ~2.9 Å; O(diethanolamine)…O(phenol), ~3.0 Å; O(diethanolamine)…O(oxime), ~2.7 Å; O(diethanolamine)…O(TMA), ~3.0 Å; O(diethanolamine)…O(MeOH), 2.894 Å. Closer inspection reveals eight O(diethanolamine)…O(diethanolamine) H-bonding interactions per cage, with the N-atoms of the same moiety all H-bonded to the phenolic O-atoms of the same ligand (N…O, ~2.65 Å). Both indicate the presence of shared protons, suggesting assignment of eight H_3L^- and four H_2L^{2-} ligands. The edges of the tetrahedron (the inter-triangle Mn…Mn distances) are approximately 7.6-7.7 Å in length, with the internal volume of the cage measuring ~57 $Å^3$ and occupied by highly disordered solvent (MeOH, H_2O) molecules. The shortest inter-cluster contacts are of the order ~3.2 Å between C-atoms of the diethanolamine arms and C-atoms of the Ph rings (Figure S1).

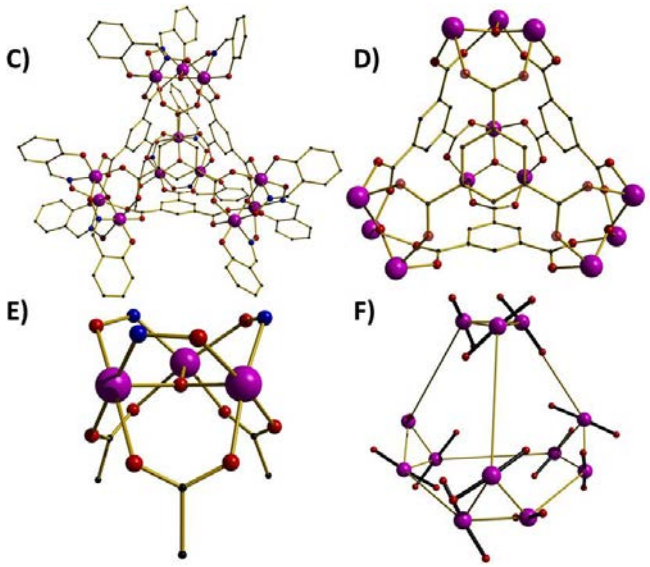

Figure 2. (C) The molecular structure of **1** with the diethanolamine moieties, peripheral C and H atoms removed for clarity. (D) The truncated tetrahedron highlighting the [Mn_3O] triangles linked by the tricarboxylates. (E) The [Mn_3O] triangular building block showing the bridging modes of the ligands. (F) The metallic skeleton highlighting both the truncated tetrahedron and the position of the Jahn-Teller axes highlighted in black. Colour code: Mn = purple, O = red, N = blue, C = grey.

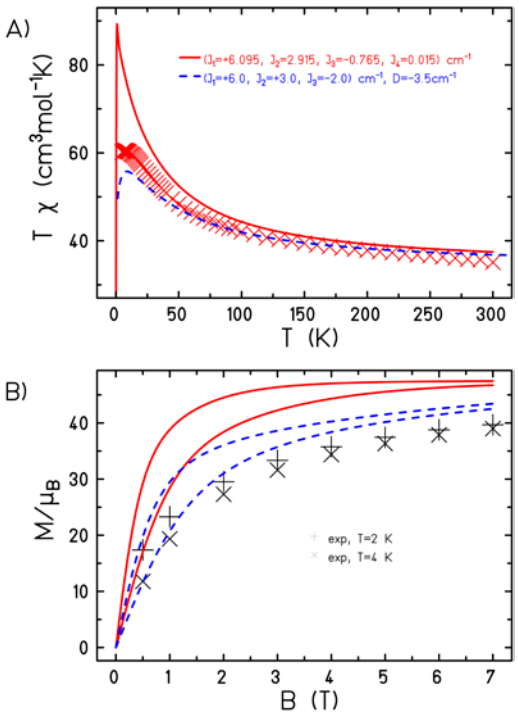

Figure 3. (A) The magnetic susceptibility of **1** at B=0.1 T (experimental data represented by crosses) and two simulations using g=1.98. The solid curves are evaluated using the Heisenberg part of the Hamiltonian with parameters from DFT; the dashed curves are produced with a Hamiltonian that includes single-ion anisotropy, but only for a fragment. (B) The magnetisation at T=2 K and T=4 K; curves are for the models mentioned in (A).

The formation of **1** was serendipitous in nature – the alcoholic arms of the diethanolamine moieties being uninvolved in bonding to the metal centres - and our initial aim was to link the [Mn_3oxime] units together *via* these alkoxide bridges. But it is clear that they must play an important structure-directing role, since the same reaction that produces complex **1**, but with H_4L replaced with a simple phenolic oxime (R-saoH_2; *i.e.* H_4L minus the diethanolamine moiety) results in the formation of a 2D framework of [Mn_6oxime] Single-Molecule Magnets (SMMs).[18] At this early juncture we can only speculate that the extensive H-bonding interactions are the cause. This itself is an interesting observation however and suggests that when synthetic chemists are designing bridging ligands they should think not only of the functional groups to be employed in linking the metal centres together, but also in the decoration of the organic framework that will eventually constitute the peripheral skin of the final complex, directing, or at least influencing, intra- and inter-molecular interactions and the packing and organisation of the molecules in the crystal.

Molecules adopting Archimedean topologies have long held fascination for chemists and physicists because of the unusual magnetic properties they often display, a beautiful example being the [Fe_{30}] icosidodecahedron which has been the subject of numerous papers.[19] A search of the CSD reveals there to be no previously reported examples of any [Mn_{12}] truncated tetrahedra in the literature with the only other examples of Mn cages adopting Archimedean geometries being a [Mn_{32}] truncated cube built with tripodal alcohols[20] and a [Mn_{12}] cuboctahedron constructed from phosphonates.[21] The magnetic susceptibility (χ) of **1** was measured from 300 K to 5 K in an applied field of 0.1 T and the results are plotted as the χT product versus T in Figure 3. The χT value of ~34.5 cm^3 K mol^{-1} at 300 K is slightly below that expected for twelve non-interacting Mn^{III} ions (36 cm^3 K mol^{-1} for g = 2). This value increases steadily as the temperature is decreased, reaching a maximum of 58.7 cm^3 K mol^{-1} at 7.5 K, before dropping slightly to a value of 58.3 cm^3 K mol^{-1} at 5 K. This behaviour is suggestive of the presence of competing ferro- and antiferromagnetic exchange interactions. The low-temperature magnetisation (Figure 3) rises to a value of ~39.7 μ_B at 7 T, lower than the saturation value (48 μ_B for g = 2.0) expected for twelve Mn^{III} ions. Modelling the experimental magnetic data of **1** *via* a standard spin Hamiltonian approach is computationally impossible, and thus we have turned to theory. DFT calculations (see the ESI for details; 5940 basis functions) were performed to estimate the intra-(J_1-J_3) and inter-(J_4) triangle interactions, yielding J_1= +6.09 cm^{-1}, J_2=+2.92 cm^{-1}, J_3= -0.77 cm^{-1} and J_4= +0.02 cm^{-1}. The latter is clearly very weak and near-negligible, as might be expected for the trimesate anion.[22]

Within the triangle the magnetic coupling is mediated *via* a μ_3-O^{2-} ion, an -N-O- oxime bridge and a carboxylate. The pertinent structural factors dominating the sign and magnitude of the exchange interactions, extracted from DFT, are listed in Table S2. J_1 is moderately ferromagnetic because both the Mn-O-Mn angle and Mn-N-O-Mn torsion angle are large. J_2 and J_3 are much weaker in magnitude, the former being ferromagnetic and the latter antiferromagnetic. The switch in sign correlates to the d_z^2-d_z^2 overlap which contributes to the AF part of the exchange, and is found to be significant for J_3 but negligible for J_2 (Tables S3-4). In the main, this is due to the orientation of the d_z^2 orbitals and the variation in the structural parameters associated with these orbitals (Table S2, Figure S5): here the d_z^2 orbitals are aligned along the carboxylate bridge (which are often responsible for counter-complementarity effects[23]) and the variation in the Mn-O_{carb} distances plays a critical role in influencing the overlap integral and thus the observed *J* values. The computed spin density plot for the high spin state of complex **1** is shown in Figure 4. Spin density analysis reveals a mixture of spin delocalisation and polarisation in operation between neighbouring Mn^{III} ions leading to weak F/AF coupling within the [Mn_3] triangle. Between the triangles however the exchange is propagated predominantly *via* spin polarisation (Figure S3), and the odd number of spacer atoms present (the carboxylates are at positions 1, 3 and 5 on the phenyl ring) results in ferromagnetic exchange coupling, albeit very weak.[24]

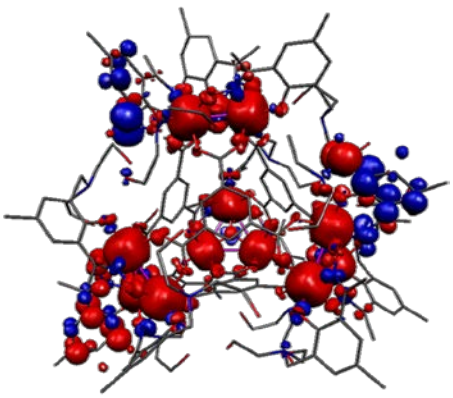

Figure 4. DFT computed spin density plot for the HS state of complex **1.** Red = positive spin density, blue = negative spin density.

To examine whether the DFT-estimated exchange coupling constants satisfactorily simulate the experimental data, we have employed the Finite-Temperature Lanczos Method.[25] This approximate method can deal with very large Heisenberg systems, therefore we could not include the single ion anisotropy terms for the Jahn-Teller active Mn^{III} ions at this point, see the solid curve in Fig. 3. Anisotropy is taken into account later for fragment calculations in a simplified way by considering the dominant part of the local anisotropy tensors (*d*-term) with site-dependent directions, $\boldsymbol{e_i}$, but with the same strength for all ions. The structure of this Hamiltonian is given in Eq. (1).[26]

$$\hat{\boldsymbol{H}} = -2\sum_{i<j}^{N} \boldsymbol{J}_{ij}\,\hat{\boldsymbol{s}}_i \cdot \hat{\boldsymbol{s}}_j + \sum_{i}^{N} \boldsymbol{d}_i\,(\boldsymbol{e}_i \cdot \hat{\boldsymbol{s}}_i)^2 + \boldsymbol{g}\boldsymbol{\mu}_B \boldsymbol{B}\sum_{i}^{N} \hat{\boldsymbol{s}}_i^{\boldsymbol{z}} \quad (1)$$

The spectroscopic splitting factor assumes a value of g=1.98. Due to the huge dimension of the Hilbert space (244,240,625) an exact eigenvalue determination including anisotropy and thus a subsequent determination of the parameters by fitting to the observables is impossible.[27] Since J_4 can be assumed to be negligible in a first approximation we have performed full diagonalisation studies, *i.e.* all eigenvalues and vectors, assuming four uncoupled identical triangles with single-ion anisotropy. The orientations $\boldsymbol{e_i}$ were chosen to be mutually perpendicular in each triangle as derived from the orientation of the Jahn-Teller axes from the single crystal X-ray structure as shown in Fig. 2F, and powder averaging was applied.[28] The curves, depicting various scenarios for J_1-J_3, and $\boldsymbol{d_i} = \boldsymbol{D}$, in Figs. 3 and S7 do not represent fits, since this is impossible, but are intended to *qualitatively* estimate the order of magnitude of exchange and anisotropy. It is clear that the parameters found by DFT lead to a reasonable χT dependence, but overestimate the low-temperature magnetisation due to the lack of anisotropic terms in the model employed. Our conclusion therefore is that two (stronger) ferromagnetic and one (weaker) antiferromagnetic exchange interactions are present in each triangle, and that the anisotropy assumes values that are typical for Mn^{III} ions.

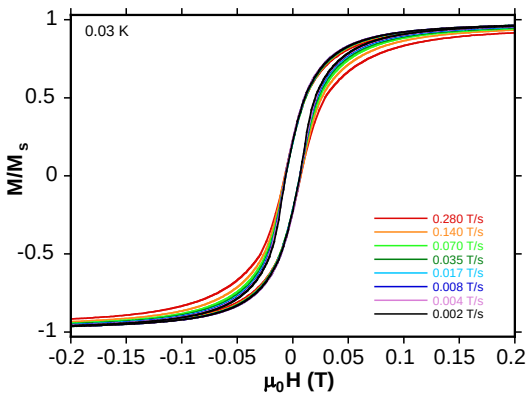

Figure 5. Magnetisation (M) versus field hysteresis loops for a single crystal of **1** at the indicated temperatures (top) and field sweep rates (bottom). M is normalised to its saturation value.

Ac susceptibility studies carried out on crystalline samples of **1** in the 1.8–10.0 K range in a 3.5 G field oscillating at frequencies up to 1000 Hz (Figure S6) display the tails of frequency-dependent out-of-phase (χ'') signals suggestive of SMM behaviour but no peaks. Hysteresis loop measurements were therefore carried out on single crystals using a micro-SQUID assembly with the field applied along the easy axis of magnetisation.[29] These show temperature and sweep rate dependent hysteresis loops confirming SMM behaviour (Figure 5). The loops are indicative of an SMM with with a modest anisotropy barrier, no significant intercluster interactions and one in which many excited states are mixed with the ground state. Low temperature dc relaxation data recorded between 0.03 – 1.00 K reveal non-exponential behaviour consistent with [multiple] excited state involvement in the relaxation process, rendering any meaningful assignment of an anisotropy barrier height impossible.

Conclusions

In conclusion, the use of the novel pro-ligand H_4L combining the complimentary phenolic oxime and diethanolamine moieties in one organic framework, has resulted in the formation of the first example of a [Mn^{III}_{12}] truncated tetrahedron and an extremely rare example of a Mn cage conforming to an Archimedean solid. The formation of such an aesthetically beautiful cage, despite the diethanolamine moieties being non-bonded, suggests synthetic variation should lead to a plethora of beautiful and novel polymetallic clusters possessing fascinating physical properties. Replacement of the trimesate ion

with redox-active congeners, if possible, will enable both stronger inter-triangle magnetic interactions and open the door to the possibility of switching the interaction on and off *via* chemical and electrochemical stimuli.

Notes and references

[a]EaStCHEM School of Chemistry, The University of Edinburgh, West Mains Road, Edinburgh, EH93JJ, UK E-mail: ebrechin@staffmail.ed.ac.uk; Paul.Lusby@ed.ac.uk
[b]Universität Bielefeld, Fakultät für Physik, Postfach 100131, 33501 Bielefeld,Germany, Email: jschnack@uni-bielefeld.de
[c]Department of Chemistry, Indian Institute of Technology Bombay, Powai, Mumbai – 400 076, India
[d]Institut Néel, 25 Avenue des Martyrs, BP 166, 38042 Grenoble, Cedex 9, France. Email: wolfgang.wernsdorfer@grenoble.cnrs.fr
UK National Crystallographic Service, Faculty of Natural and Environmental Sciences, University of Southampton, SO171BJ, Southampton, UK. Email: M.Pitak@soton.ac.uk; s.j.coles@soton.ac.uk

Electronic Supplementary Information (ESI) available: synthetic procedures, crystallographic details and additional magnetic and theoretical data. See DOI: 10.1039/c000000x/

1 G. Aromí and E. K. Brechin, *Struct. Bonding*, 2006, **122**, 1-69.
2 G. Aromí, D. Aguilà, P. Gamez, F. Luis and O. Roubeau, *Chem. Soc. Rev*., 2012, *41*, 537-546.
3 M. Andruh, *Chem. Commun*., 2011, **47**, 3025-3042.
4 V. Marvaud, C. Decroix, A. Scuiller, C. Guyard-Duhayon, J.Vaissermann, F. Gonnet and M. Verdaguer, *Chem. Eur. J*., 2003, **9**, 1677-1691.
5 F. Habib and M. Murugesu, *Chem. Soc. Rev*., 2013, **42**, 3278-3288.
6 L. N. Dawe, K. V. Shuvaev and L. K. Thompson, *Chem. Soc. Rev*. 2009, **38**, 2334-2359.
7 T. Glaser, *Chem. Commun*., 2011, **47**, 116-130.
8 C. J. Milios, T. C. Stamatatos and S. P. Perlepes, *Polyhedron*, 2006, **25**, 134-194.
9 (a) G. A. Timco, E. J. L. McInnes and R. E. P. Winpenny, *Chem. Soc. Rev*., 2013, **42**, 1796-1806; (b) G. A. Timco, T. B. Faust, F. Tuna and R. E. P. Winpenny, *Chem. Soc. Rev*., 2011, **40**, 3067-3075.
10 R. Bagai and G. Christou, *Chem. Soc. Rev*., 2009, **38**, 1011-1026.
11 R. Sessoli and A. K. Powell, *Coord. Chem. Rev*., 2009, **253**, 2328-2341.
12 M. Murrie, *Chem. Soc. Rev*., 2010, **39**, 1986-1995.
13 X.-Y. Wang, C. Avendaño and K. R. Dunbar, *Chem. Soc. Rev*., 2011, **40**, 3213-3238.
14 K. S. Murray, *Aust. J. Chem*., 2009, **62**, 1081-1101.
15 a) R. Inglis, C. J. Milios, L. F. Jones, S. Piligkos and E. K. Brechin, *Dalton Trans*., 2012, **48**, 181-190; b) R. Inglis, L. F. Jones, C. J. Milios, S. Datta, A. Collins, S. Parsons, W. Wernsdorfer, S. Hill, S. P. Perlepes, S. Piligkos and E. K. Brechin, *Dalton Trans*., 2009, 3403-3412; c) C. J. Milios, S. Piligkos and E. K. Brechin, *Dalton Trans*., 2008, 1809-1817.
16 a) A. J. Tasiopoulos and S. P. Perlepes, *Dalton Trans*., 2008, 5537-5555; b) R. W. Saalfrank, A. Scheurer, R. Prakash, F. W. Heinemann, T. Nakajima, F. Hampel, R. Leppin, B. Pilawa, H. Rupp and P. Müller, *Inorg. Chem*., 2007, **46**, 1586-1592.
17 T. C. Stamatatos, D. Foguet-Albiol, S.- C. Lee, C. C. Stoumpos, C. P. Raptopoulou, A. Terzis, W. Wernsdorfer, S. O. Hill, S. P. Perlepes and G. Christou, *J. Am. Chem. Soc.*, 2007, **129**, 9484–9499.
18 A. D. Katsenis, R. Inglis, A. Prescimone, E. K. Brechin and G. S. Papaefstathiou, *CrystEngComm*., 2012, **14**, 1216-1218.
19 U. Kortz, A. Müller, J. van Slageren, J. Schnack, N. S. Dalal and M. Dressel, *Coord. Chem. Rev*., 2009, **253**, 2315-2327.
20 R. T. W. Scott, S. Parsons, M. Murugesu, W. Wernsdorfer, G. Christou and E. K. Brechin, *Angew. Chem. Int. Ed*., 2005, **44**, 6540-6543.
21 L. Zhang, R. Clérac, P. Heijboer and W. Schmitt, *Angew. Chem. Int. Ed*., 2012, **51**, 3007-3011.
22 P. Christian, G. Rajaraman, A. Harrison, M. Helliwell, J. J. W. McDouall, J. Raftery and R. E. P. Winpenny, *Dalton Trans*. 2004, 2550-2555.
23 M. Atanasov, B. Delley, F. Neese, P. L. Tregenna-Piggott and M. Sigrist, *Inorg. Chem.*, 2011, **50**, 2112-2124.
24 J. Cano, E. Ruiz, S. Alvarez and M. Verdaguer, *Comments Inorg. Chem*., 1998, **20**, 27-56.
25 a) J. Jaklič and P. Prelovšěk, *Phys. Rev. B*. 1994, 49, 5065; b) J. Schnack and O. Wendland, *Eur. Phys. J. B*. 2010, **78**, 535-541; c) J. Schnack, C. Heesing, *Eur. Phys. J. B* 2013, **86**, 46
26 a) T. Glaser, M. Heidemeier, E. Krickemeyer, H. Bögge, A. Stammler, R. Fröhlich, E. Bill and J. Schnack, *Inorg. Chem.*, 2009, **48**, 607-620; b) J. Schnack, *Condens. Matter Phys.*, 2009, **12**, 323-330.
27 V. Hoeke, M. Heidemeier, E. Krickemeyer, A. Stammler, H. Bögge, J. Schnack, A. Postnikov and T. Glaser, *Inorg. Chem.*, 2012, **51**, 10929-10954.
28 V. I. Lebedev and D. N. Laikov, *Dokl. Akad. Nauk.* 1999, **366**, 741-745.
29 a) W. Wernsdorfer, *Adv. Chem. Phys*., 2001, **118**, 99–190; b) W. Wernsdorfer, *Supercond. Sci. Technol*., 2009, **22**, 064013/1–064013/13.